

Superconducting Phase Diagram of UPt_3 , Studied by Thermal Expansion and Specific Heat

K. Hasselbach,* A. Lacerda, K. Behnia, L. Taillefer, and J. Flouquet

Centre de Recherches sur les Très Basses Températures, CNRS, Grenoble, France

and

A. de Visser

Natuurkundig Laboratorium der Universiteit van Amsterdam, Amsterdam, The Netherlands

(Received July 18, 1990)

The specific heat and thermal expansion of UPt_3 were measured in the vicinity of the superconducting transition for magnetic fields up to 10 kOe, applied along the hexagonal c axis. Both thermodynamic techniques show clear evidence of two transitions in zero field, which merge at a critical field of approximately 8 kOe. The upper critical field curve determined by the resistivity for the upper transition exhibits a small but abrupt change of slope at a comparable value of the field. The phase diagram that emerges for $H\parallel c$ is therefore qualitatively similar to that previously found for $H\perp c$, this time with a critical point (or region) around $H^ = 8$ kOe, $T^* = 0.36$ K. The implications of a nearly isotropic phase diagram are discussed in connection with recent theories.*

1. INTRODUCTION

The occurrence of superconductivity in the class of intermetallic compounds with highly correlated electrons known as "heavy-fermion metals" has intrigued many researchers over the past decade. Much of the interest arises from the fact that the superconducting condensate is formed by electrons with heavily renormalized masses. Since the renormalization is thought to involve predominantly spin rather than charge or phonon degrees of freedom, a pairing mechanism based on magnetic fluctuations is envisaged. However at present, there is still no convincing microscopic model to confirm this speculation.

Nevertheless, the unconventional nature of the superconducting state in these compounds makes little doubt when one considers the symmetry

*Permanent address: Physikalisches Institut der Universität Karlsruhe, Federal Republic of Germany.

of the order parameter. In the case of UPt_3 , perhaps the most thoroughly investigated of the four heavy-fermion superconductors (largely because of the availability of high-quality, single-crystalline samples), two types of experimental evidence have revealed an unusual order parameter. First, almost immediately after superconductivity was discovered¹ in UPt_3 , it has been suggested that the nonexponential temperature dependence of various physical properties in the superconducting state, such as the ultrasonic attenuation,² specific heat,³ thermal conductivity,⁴ and NMR relaxation rate,⁵ evidenced the presence of zeros in the gap function.

Recently, a second kind of evidence for an unconventional order parameter has come to the fore as anomalies indicative of additional transitions *within* the superconducting regime. The earliest hint came from a sharp break, or “kink,” in the slope of the upper critical field curve⁶ (see also Ref. 7), followed by the observation of a peak in the field dependence of the ultrasonic attenuation⁸ (see also Refs. 9 and 10) and then in the last year by a host of other “signatures.” Among the evidence gathered so far, perhaps the most compelling are the two clear discontinuities in the temperature dependence of the specific heat^{11,12} at T_c^- and T_c^+ , separated by 60 mK in zero magnetic field (i.e., about 10% of T_c^+).

Such a double-peak structure has been observed also in UBe_{13} when this compound is doped with approximately 3% of thorium.¹³ Apart from the uncertainty regarding the role of Th impurities in bringing about a second transition, the main points of difference with UPt_3 are the cubic symmetry of the crystal structure, the absence of a well-defined Fermi liquid behavior above T_c , and the large separation of the two transitions (up to 35% of T_c), in $(\text{U, Th})\text{Be}_{13}$.

Moreover, there is another particularity of UPt_3 that may influence its superconducting behavior, namely the existence¹⁴ of an antiferromagnetic order below 5 K (i.e., well above the T_c of 0.5 K). A number of recent theoretical treatments¹⁵⁻¹⁷ have attributed the presence of a second transition just below the first to the lifting of a doubly-degenerate 2D representation (in a *d*-wave superconductor). The lifting would be caused by a symmetry-breaking field, which could arise in UPt_3 , for example, from a coupling of the vector order parameter to the antiferromagnetic moment lying in the basal plane of the hexagonal crystal structure. Some experimental evidence has been presented in favor, and some against, this appealing proposal (see for example Ref. 18 and references therein), but it is still too early to draw conclusions on the true relevance of the weak antiferromagnetic order when it comes to the superconducting phase diagram.

One line of approach for the further experimental investigation of this issue, which is fundamentally tied to considerations of symmetry, is the study of anisotropy, both in the effect of a magnetic field and of lattice

deformations. In the present article, we take this approach by looking at two thermodynamic quantities in a magnetic field: the specific heat and the thermal expansion coefficient along the different axes. These are both second derivatives of the Gibbs potential and as such rigorously connected through thermodynamic rules like the Ehrenfest relation for second-order phase transitions.

2. EXPERIMENTAL RESULTS

All measurements presented here were performed on single crystals prepared under similar conditions: from a highly-purity batch of UPt_3 in an induction furnace under ultra-high vacuum. The specimens for specific heat and thermal expansion were spark-cut out of a rod containing large grains. The rod was produced by slow unidirectional cooling in the water-cooled copper crucible of a horizontal zone-refiner. The specimen for resistivity is a whisker which grew spontaneously out of the melt upon quenching.

2.1. Specific Heat

The heat capacity was measured by a heat-pulse relaxation technique described in Ref. 12, in which the sample is mounted on a silicon plate that also supports the phosphor-doped silicon thermometer. The magnetic field is applied parallel to the c axis of the single-crystalline, disklike sample that makes an angle of 25° with the plane of the disk. This same sample was used for the $H \perp c$ study published previously.¹² The contribution from the sample holder itself is inferior to 3% of the total heat capacity at 0.5 K and is therefore ignored in the present analysis.

The specific heat of UPt_3 in the temperature interval 0.25–0.55 K and for magnetic fields up to 10 kOe, applied along the c axis, is shown in Fig. 1 (see also Ref. 19). The presence of two discontinuities is readily established, in particular at zero field where the width of the transitions (approximately 15 mK) is much less than the separation between them. Using an idealized construction (as shown for the data at $H = 0$), T_c^- and T_c^+ are defined as the positions of the sharp drop for the lower and the upper transitions, respectively. For $H = 0$, their values are $T_c^- = 0.434$ K and $T_c^+ = 0.490$ K, with a relative accuracy of ± 2 mK, so that $\Delta T_c \equiv T_c^+ - T_c^- = 56 \pm 4$ mK.

As the magnetic field is increased, these two transitions converge, i.e., ΔT_c decreases, in a manner given in Ref. 12 and $H \perp c$ and shown here for $H \parallel c$. The overall behavior is rather similar in the two configurations, with a complete merging (or at least indistinguishability) of T_c^+ and T_c^- taking place at a field value H^* between 5 and 6 kOe for $H \perp c$, and between 7

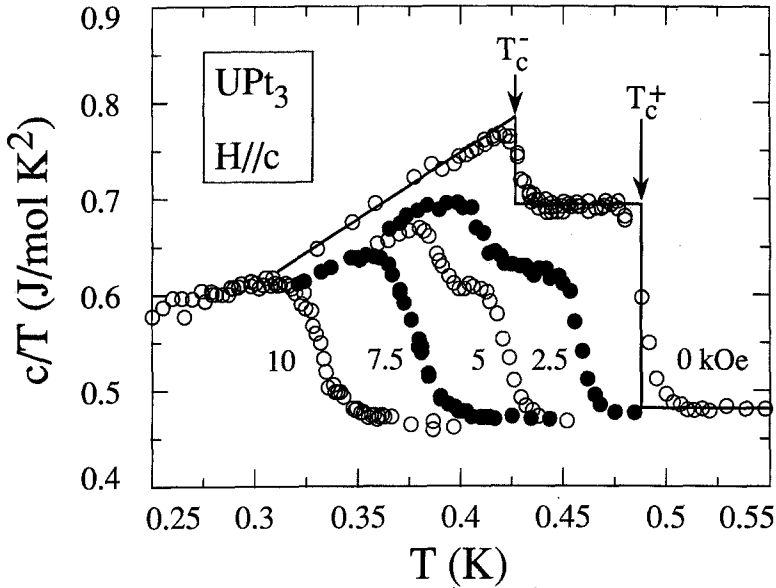


Fig. 1. Specific heat of UPt_3 as a function of temperature, plotted as c/T vs T , for magnetic fields H from 0 to 10 kOe in steps of 2.5 kOe, applied along the hexagonal c axis. Note the two-well resolved discontinuities which converge as the field is increased. The solid line is an idealized construction used to define the lower and upper critical temperatures T_c^- and T_c^+ (shown here only for $H=0$).

and 8 kOe for $H \parallel c$. This corresponds to a merging temperature T^* equal to 380 and 360 mK, respectively. Note that for $H > H^*$, only one discontinuity is resolved, and consequently the idealized construction used to define (a single) T_c consists of only one drop. The detailed evolution of $T_c^+(H)$ and $T_c^-(H)$ defined in this way translates as two liners in the $H-T$ phase diagram (Fig. 6), which we discuss in Sec. 3. The initial slope of these lines is $dH_{c_2}^+/dT = -75$ kOe/K and $dH_{c_2}^-/dT = -100$ kOe/K as $H \rightarrow 0$, with a 5% accuracy.

As pointed out earlier,²⁰ the upper transition is seen to be more sensitive both to the strength of the field ($dH_{c_2}^+/dT > dH_{c_2}^-/dT$) and to its orientation; indeed for $H \perp c$, $dH_{c_2}^+/dT = -43$ and $dH_{c_2}^-/dT = -95$ kOe/K, with the same accuracy.¹² In our constant-field curves, the last to reveal clearly a double structure is that for which $H = 6.25$ kOe, where $\Delta T_c \sim 25$ mK. Beyond that field, the width of the overall transition (~ 15 mK) becomes comparable to the separation, limiting further resolution.

Ellman and co-workers have recently presented specific heat²¹ data on UPt_3 for $H \parallel c$. The sample they used for their measurement is not such as to have allowed for a resolution of the two discontinuities: indeed, only a

single broad transition is seen (with full width of order 100 mK, while $T_c^+ - T_c^-$ is known to be about 60 mK^{11,12}). As a consequence, their work has little overlap with ours.

Nevertheless, these authors claim to identify a second transition line in the $H - T$ plane that would run roughly parallel to the first. The first, in this case, was given by the onset of superconductivity, i.e., by the point (H, T) at which the specific heat starts to increase above its normal-state value. The second line comes out to be 100 to 200 mK below. In our opinion, this second line may be an artefact of their analysis based on constant temperature sweeps, and it corresponds to a reproduction of the first $H_{c_2}(T)$ line, obtained with a different criterion.

2.2. Thermal Expansion

The coefficient of linear thermal expansion $\alpha = L^{-1} dL/dT$ was measured along the a and the c axis of a single crystal cut in the shape of a rectangular bar with dimensions $a \times b \times c \approx 2 \times 1 \times 3 \text{ mm}^3$ (this is sample 2 of Ref. 22). Changes in length L were measured by way of a three-terminal-capacitance method, using a capacitance bridge developed in Grenoble, at the Centre de Recherches sur les Très Basses Températures. The use of a low-temperature preamplifier and of a low-temperature reference capacitor has led to an improved sensitivity with respect to the data of Ref. 22, with a detection limit now at $\Delta L/L = 2 \times 10^{-10}$. The sample was placed in a capacitance cell²³ machined out of oxygen-free, high-conductivity copper. A heater and a Matsushita resistor used as a thermometer were attached directly to the sample with G.E. varnish. Data points were gathered by temperature modulation of the sample ($f \sim 0.1 \text{ Hz}$, $\Delta T \approx 5 \text{ mK}$) while the cell was kept at constant temperature. Since the sample was in thermal contact with the cell, any volume change in the latter affected the signal. This made it difficult to establish an absolute calibration. However, comparing the present data with the previously published absolute data,²² it appeared that the contribution of the cell to the measured signal is small (with an expansion coefficient always less than $4 \times 10^{-7} \text{ K}^{-1}$) and featureless in the temperature interval of interest. Therefore, the cell contribution was not subtracted from the data. This allows only for an approximate numerical analysis; on the other hand, most of our conclusions do not depend on absolute values.

The temperature dependence of the linear thermal expansion in the vicinity of the superconducting transition is shown in Fig. 2, for length changes parallel and perpendicular to the hexagonal axis, in the absence of a magnetic field. In this temperature range (0.3–0.6 K), the behavior is anisotropic in two ways: first, the basal plane expands upon heating ($\alpha_{\perp} > 0$),

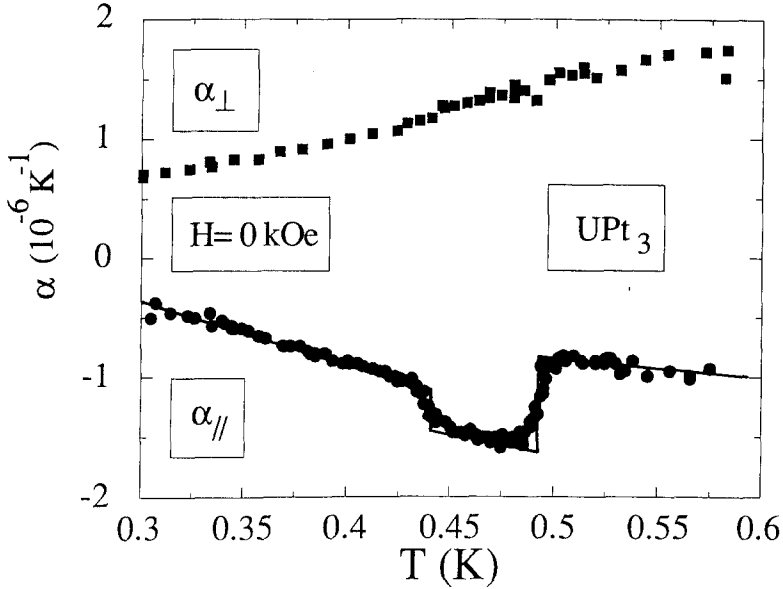


Fig. 2. Coefficient of linear thermal expansion of UPt_3 parallel (α_{\parallel}) and perpendicular (α_{\perp}) to the hexagonal axis, as a function of temperature, in zero magnetic field. Note the two discontinuities in α_{\parallel} at $T_c^- = 442$ mK and $T_c^+ = 494$ mK, defined using the idealized construction shown by the solid line. (The data have not been corrected for the cell effect, so the absolute scale is only approximate).

while the c axis contracts ($\alpha_{\parallel} < 0$), and second, the appearance of superconductivity affects the response along c much more than the response along a or b . Indeed at the onset of superconductivity (around 490 mK), an abrupt increase in $|\alpha_{\parallel}|$ is observed, whereas a kink occurs for α_{\perp} .²² Using the Ehrenfest relation, it could be concluded that the anisotropy in the discontinuities in α at T_c implies that an uniaxial pressure along the c axis strongly depresses T_c , while a stress along the a axis will hardly influence T_c . This is consistent with the result of Greiter and co-workers²⁴ who found that the onset of superconductivity (which would correspond to T_c^+ , as it was measured by ac susceptibility) was rapidly suppressed by uniaxial compression of the c axis, at a linear rate of $dT_c/d\varepsilon = -26$ mK/kbar, while stress along either the a or the b axis produced no detectable effect (up to $\varepsilon = 0.8$ kbar)^{20,24}.

Of particular interest here is the clear evidence for a second low-temperature transition, as seen in both α_{\parallel} and α_{\perp} (yet much more clearly in the former). By using the idealized construction drawn for α_{\parallel} in Fig. 2, two transition temperatures may be defined: $T_c^- = 442$ mK and $T_c^+ = 494$ mK, with a relative accuracy of ± 4 mK. These anomalies are obviously to be

identified with the two discontinuities in the specific heat. The coefficient of volume expansion $\alpha_v = \alpha_{\parallel} + 2\alpha_{\perp}$ is obtained by adding the two curves of Fig. 2, using interpolated values for $\alpha_{\perp}(T)$, which correspond to the actual data points of $\alpha_{\parallel}(T_i)$, for every T_i . The result is shown in Fig. 3. The quantitative behavior is clear-cut: α_v decreases abruptly at T_c^+ (still remaining positive), while its change at T_c^- is at least one order of magnitude smaller. Given that the specific heat exhibits a large discontinuity at that transition, this implies that T_c^- is much less sensitive to changes in volume.

More quantitatively, the Ehrenfest relation

$$\left. \frac{dT_c}{dP} \right|_{P=0} = \frac{V_m T_c \Delta\alpha_v}{\Delta c_p} \quad (1)$$

(where V_m is the molar volume and $\Delta\alpha_v$ and Δc_p are the discontinuities at T_c) allows us to derive the (hydrostatic) pressure dependence of the two transition temperatures T_c^+ and T_c^- (see Ref. 22). For an analysis in terms of Eq. (1), it is important to bear in mind that a measure of dT_c/dP is needed at *small* pressures (ideally, in the limit of zero pressure) and that the pressure dependence of T_c (as measured by resistivity) undergoes a

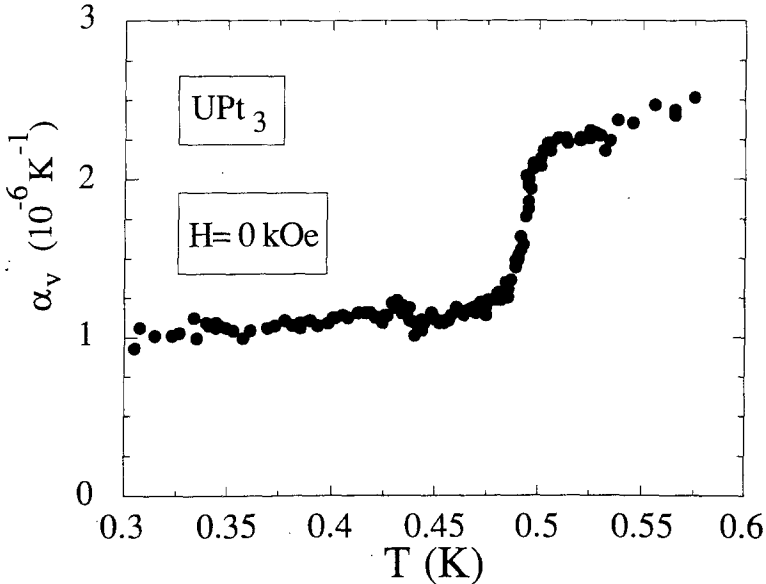


Fig. 3. Volume thermal expansion coefficient of UPt₃, defined as $\alpha_v = \alpha_{\parallel} + 2\alpha_{\perp}$, as a function of temperature in zero magnetic field. Note the contrast between the large (and narrow) drop at T_c^+ , with $\Delta\alpha_v(T_c^+) \cong -1 \times 10^{-6} \text{ K}^{-1}$, and the virtual absence of any anomaly at T_c^- ($=442 \text{ mK}$). The latter fact suggests an insensitivity of T_c^- to applied pressure. (As for Fig. 2, the absolute scale is only approximate).

considerable change of regime around 2 kbar, going from a fast rate of decrease (-24 mK/kbar) over to a much slower rate (-13 mK/kbar), as established by the resistive measurements of Behnia and co-workers.²⁵ We know of three pressure studies of T_c performed below 2 kbar (at $H = 0$): (1) the resistive measurements just quoted, which yield $dT_c^+/dP = -24$ mK/kbar, (2) the stress experiments²⁰ cited above which yield an overall $dT_c^+/dP = -26$ mK/kbar, and (3) the preliminary specific heat study of Trappmann and co-workers²⁶ who find a value in agreement with these figures for T_c^+ and furthermore a much weaker dependence on hydrostatic pressure for T_c^- .

In view of the large anisotropy of the effect of lattice deformation on the superconducting behavior, some caution is required when comparing experiments performed on different samples (with different manometry and thermometry) using different pressure-transmitting media at low temperature (alcohol in particular). However, the convergence of all three estimates onto the same value of -25 mK/kbar to within 10% is reassuring.

From Fig. 1, the size of the jump in specific heat at the upper transition is $\Delta c_p/T_c^+ = 0.22$ J K⁻² mol⁻¹. From Fig. 3, the *negative* jump in α_v is approximately 1×10^{-6} K⁻¹ (with a 10% uncertainty). With a molar volume²³ of 4.244×10^{-5} m³ mol⁻¹, we get $dT_c^+/dP = -20 \pm 3$ mK/kbar. Within the error bars, this agrees with the measured value, and the Ehrenfest relation is roughly satisfied, at least at $H = 0$.

The influence of a magnetic field H applied along the c axis on the anomalies in α_{\parallel} is shown in Fig. 4, for $H = 0.0, 2.5, 5.0,$ and 7.5 kOe. Using idealized constructions of the kind shown in Fig. 2 to define a T_c^- and a T_c^+ for each field, we get: $T_c^+(H) = 492, 462, 424, 378$ mK and $T_c^-(H) = 439, 419, 390, 363$ mK for $H = 0.0, 2.5, 5.0, 7.5$ kOe, respectively. Two transition lines are then obtained in an $H - T$ phase diagram, as drawn in Fig. 6, which converge at roughly $H^* = 8$ kOe. Note that because the discontinuities in α_{\parallel} at T_c^- and T_c^+ are of opposite sign while the corresponding discontinuities in c_p are of the same sign, the thermal expansion data allows for a finer resolution of the two transitions even though the widths are comparable for the two techniques (i.e., about 15 mK). Before we come to a discussion of that phase diagram (in Sec. 3), a few points must be emphasized. Although Eq. (1) cannot strictly be used to analyze the results of Fig. 4, since at the moment data for α_{\perp} at finite fields is lacking, it is interesting to note that, at the upper transition, the jump in α_{\parallel} (which is equal to $\Delta\alpha_v$ when $H = 0$) scales with $\Delta c_p/T_c^+$ as the field is increased, suggesting that dT_c/dP remains roughly constant (with its large negative value). This would be in sharp contrast with the results of Behnia and co-workers²⁵ on the hydrostatic pressure dependence of the resistive transition performed with $H_{\perp}c$, who find that on the contrary, for that field direction dT_c/dP (at small

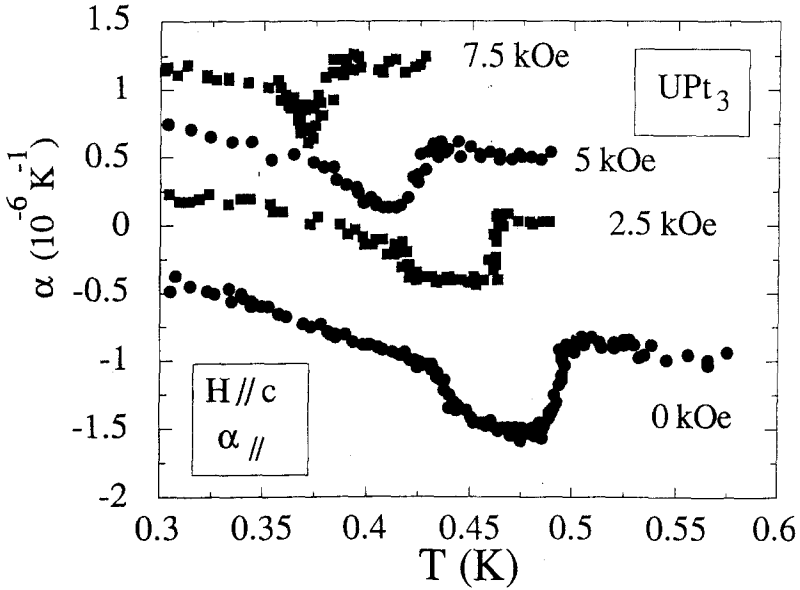


Fig. 4. Temperature dependence of the coefficient of linear thermal expansion α_{\parallel} for different values of the the magnetic field applied along the c axis, as indicated. (The three upper curves have been shifted upwards for the sake of clarity, thereby making the zero of the vertical axis arbitrary). The transition temperatures are defined using constructions of the kind shown in Fig. 2.

pressures) varies considerably with field, perhaps even changing sign at $H \sim 5$ kOe. This contrasting situation would seem to point either to a large anisotropy in the field dependence of dT_c/dP (at $P = 0$) (and hence of $\Delta\alpha_v$) or to the growth with field of a positive jump in α_{\perp} at T_c^+ , which would eventually overcompensate $\Delta\alpha_{\parallel}$. To elucidate this state of affairs, more measurements are needed, especially of the kind that separates effects along various crystallographic axes.

A second point concerns the detailed behavior of $\alpha_{\parallel}(T)$ in the vicinity of the two transitions. As emphasized already, the two discontinuities in α_{\parallel} at T_c^+ and T_c^- are of opposite sign, the former being negative and sharp, the latter being positive and somewhat smaller and more gradual. As the field is increased, the two $\Delta\alpha$'s decrease in amplitude roughly hand-in-hand with the decrease in the corresponding Δc_p 's (see Fig. 1), until the two transitions eventually merge at about 8 kOe. This behavior appears to change significantly when the field exceeds 8 kOe. Indeed, as a preliminary run at 10 kOe has shown, the single anomaly in α_{\parallel} expected to correspond to the single jump in c_p (Fig. 1) becomes suddenly much smaller, in fact below our current level of detection at that field (with a much increased noise

level at high fields). This suggests a sudden drop in the c axis stress dependence of T_c as the field is increased beyond H^* , and a qualitative difference in the sensitivity of H_{c2} to lattice deformations, for fields below and above the critical point.

2.3. Upper Critical Field from Resistivity

With the possibility of a critical point in the $H - T$ diagram for $H \parallel c$, it became of interest to determine the field dependence of $T_c^+(H)$ with greater precision than is possible from thermodynamic measurements by using the drop in electrical resistance at the onset of superconductivity, as was done previously for $H \perp c$.^{7,18}

The resistivity measurements were performed on a single-crystalline whisker (with its length along the c axis) of low residual resistivity ($0.1 \mu\Omega$ cm, extrapolated to $T=0$). This sample was used in previous H_{c2} measurements, from which the existence of a clear "kink" was established for a field orientation in the basal plane.^{7,18} The sample, heater, and RuO_2 thermometer were mounted on a copper block immersed in liquid ^3He , which served as thermal link to the mixing chamber of a top-loading dilution refrigerator. Field and current were applied along the c axis. For every value of the magnetic field, the transition temperature T_c was defined as the inflection point in the resistance vs. temperature curve, the width of which was 15 mK. The resulting uncertainty on the value of $T_c(H)$ is ± 0.5 mK. The small and smooth magnetoresistance of the thermometer was not corrected for, introducing an error on the absolute value of the estimated temperature of 2 mK at the highest field (12 kOe).

The field dependence of the critical temperature defined in this way is plotted in Fig. 5, for fields up to 12 kOe. The first point to note is the high value of T_c at $H=0$, equal to 547 mK—high in two respects: (1) when compared with the resistive T_c of other (single-crystalline) samples,⁷ and (2) when compared with the T_c^+ derived from specific heat or thermal expansion measurements. The considerable discrepancy between the resistive and the thermodynamic T_c^+ , of order 50 mK, was discussed in Ref. 12; we mention it here only to point out that a direct superposition of $H_{c2}(T)$ curves obtained by these different methods is not possible.

The second point is the absence of any striking feature. Therefore, in order to establish whether a small yet abrupt change of behavior may indeed be present in the data of Fig. 5, the following procedure was used. A second-order polynomial was fitted to the points over three different field intervals: (1) low fields (0–5 kOe), (2) high fields (7–12 kOe), and (3) intermediate fields (3.5–8.5 kOe). The parabolic fits obtained have negative curvature for intervals (1) and (2) and positive curvature for (3), with a

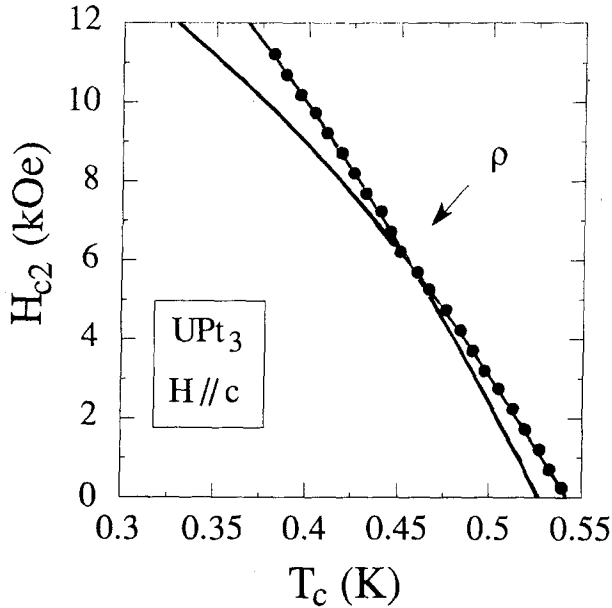


Fig. 5. Temperature dependence of the upper critical field $H_{c2}(T)$ for $H \parallel c$, as determined from the drop in resistance as a function of temperature (at $T_c(H)$). The solid lines are separate quadratic fits to the data at low and high fields, respectively. These bring out the small but abrupt change in the slope of $H_{c2}(T)$ at $H \approx 6.0$ kOe.

standard deviation of the discrepancies between data and fit (at fixed temperature) of 35, 10, and 52 Oe, respectively. The positive curvature in the middle region does point to a change of regime, and the poorer quality of the corresponding fit is consistent with the change being abrupt. As seen from Fig. 5, the H_{c2} curve departs rather suddenly from its low field behavior at 6 kOe. This unusual feature, resolvable with the accuracy of the present measurements, is indicative of a critical point on the $H_{c2}(T)$ line, in the same but less pronounced way it was for $H \perp c$. The initial slope of $H_{c2}(T)$ is -75 kOe/K, in agreement with the specific heat estimate.

3. THE H - T PHASE DIAGRAM

The two transition temperatures $T_c^+(H)$ and $T_c^-(H)$ located by both thermodynamic measurements as a function of temperature at various constant values of the field in the range 0-12 kOe are collected in the phase diagram of Fig. 6. The two sets of points obtained from thermal expansion and specific heat data are seen to be in complete agreement with each other, within experimental resolution. The two transitions, thus unambiguously

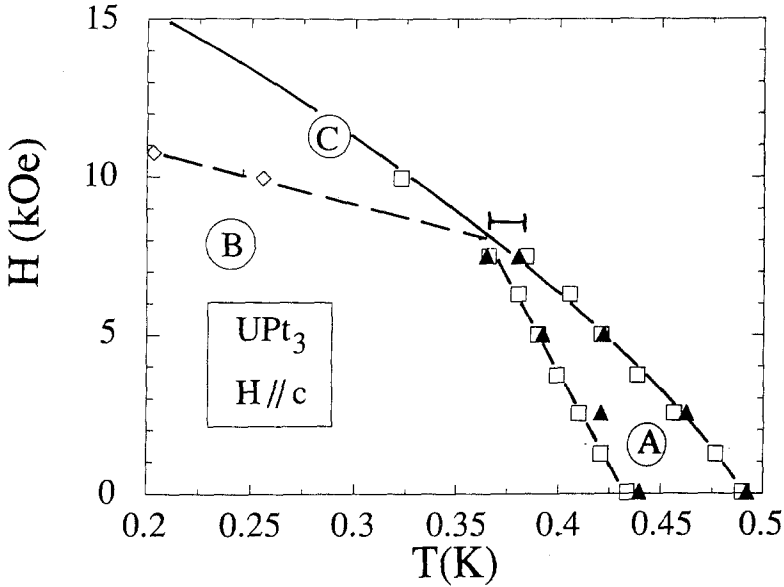


Fig. 6. Multicomponent phase diagram of superconducting UPt_3 for a magnetic field along the hexagonal axis. The open squares and the closed triangles correspond to the transition temperatures $T_c^-(H)$ and $T_c^+(H)$, as determined from the idealized constructions of Fig. 1 for the specific heat and Fig. 4 for the thermal expansion along c . Open diamonds (and the dashed line) indicate the position of a peak observed by Schenstrom and co-workers in the field dependence of the ultrasonic attenuation.¹⁰ The solid lines are guides to the eye. We have labeled the three regions of the diagram A, B, and C, as in Ref. 12.

identified, converge as the field is increased and become indistinguishable beyond about 8 kOe. This leads us to define a critical point (or region) with coordinates $H^* = 8$ kOe and $T^* = 0.36$ K. The kink in the $H_{c2}(T)$ curve of Fig. 5 is in qualitative support of this picture. However, the kink occurs significantly lower in field than H^* , namely at 6.0 kOe—a situation also encountered with the phase diagram for $H \perp c$.¹² This may not be significant, as it could be a consequence of the overall shift of the H_{c2} curve to higher temperatures when determined from resistivity as opposed to thermodynamic measurements.

The information now available on the three “thermodynamic” transition lines of the phase diagram (i.e., the solid lines of Fig. 6) is the following: (1) *the upper transition at low fields* is the most sensitive to both the amplitude of the magnetic field and to its direction (i.e., whether $H \parallel c$ or $H \perp c$), it is characterized by a large and negative $\Delta\alpha_v$ which takes place almost entirely along the c axis (at $H = 0$), so that $\Delta\alpha_{\perp} \cong 0$, and correspondingly T_c^+ is suppressed only by stress along the c axis; (2) *the lower transition at low*

fields is more or less insensitive to the orientation of the field, it exhibits negligible change in α_v as a result of a compensation between $\Delta\alpha_{\parallel}$ (which is positive) and $2\Delta\alpha_{\perp}$ (which is negative), the result being a T_c^- very weakly dependent on hydrostatic pressure; (3) *the single transition at high fields* ($H > H^*$) is not as well characterized, but it would seem to be much less affected by c axis stress than the other two.

In addition to these “thermodynamic” transitions, an extra line in the H - T diagram can be drawn, deep within the superconducting regime, on the basis of anomalies observed in a variety of dynamic measurements: ultrasonic attenuation,⁸⁻¹⁰ viscosity by torque measurements,²⁷ thermal conductivity,²⁸ and sound velocity.²⁹ For $H \parallel c$, the position of the ultrasound anomalies is shown by a dashed line in Fig. 6, separating two regions which we call B and C . So far such a line, either for $H \parallel c$ or $H \perp c$, has not been detected in any thermodynamic measurement (e.g., specific heat, thermal expansion, magnetization, etc.). In particular, our own measurement of the magnetostriction, which probes the pressure dependence of the magnetization, showed no evidence of that line. Since the magnetization at fields comparable to $H_{c2}(0)$ is mainly governed by the Pauli susceptibility of the material, it therefore seems that the latter undergoes no major change at that line. As was suggested by several authors,^{10,17,30} these anomalies may result from a vortex transition—either a rearrangement of the vortex lattice or a change in the vortex core. Any measurement sensitive to the motion of, or the scattering from, vortices would pick up this kind of transition (which may not involve a great deal of entropy). Moreover, the features observed may depend on the quality of the sample, for vortex pinning could play a role. Whether this “vortex” line intersects the $H_{c2}(T)$ curve precisely at H^* cannot yet be answered given the available information gathered from different samples using different thermometers.

In summary, the superconducting phase diagram of UPt_3 is rather isotropic—with only a small dependence on field orientation in and out of the basal plane, and it is made up of (at least) three regions (labelled A , B , and C) separated by four lines (three “thermodynamic” lines + one “vortex” line) all converging at a critical region centered around a point (H^* , T^*) on the upper critical field curve, equal to (8 kOe, 0.36 K) for $H \parallel c$ and (5 kOe, 0.37 K) for $H \perp c$. The details of the phase diagram near that point are not yet resolved.

4. DISCUSSION

A central question concerning the phase diagram of UPt_3 is the origin of the second transition at T_c^- . Among the potential explanations are the following four.

A first might be sample inhomogeneity, but it can be safely ruled out because of (1) the reproducibility of the double-structure in the specific heat when measured in different samples (see Refs. 11, 12, and 31), (2) the narrow width of the transitions which can be achieved (cf. Fig. 1), and the different response of the upper and lower transitions to (3) an applied magnetic field and particularly to (4) c axis stress. Indeed in the latter case, the two transitions move in *opposite* directions.

A second possibility is long-range magnetic order. The absence of any feature in the dc magnetization at T_c^{-32} dismisses ferromagnetism, but a very weak antiferromagnetic ordering is not as easily disqualified. The idea would be that T_c^- is in fact a Néel temperature—a second one below T_c , that is, for commensurate ordering of small moments¹⁴ ($0.02 \mu_B$) in the basal plane of UPt_3 is already known to set in well above T_c , at 5 K. The kink in $H_{c_2}(T)$ would then be akin to that found³³ in some Chevrel phases with $T_N < T_c$, as in SmRh_4B_4 , for example, where the kink indeed coincides with an antiferromagnetic order at 0.87 K, well below $T_c(0) = 2.7$ K. Although very small moments could obviously have been missed, elastic neutron experiments on UPt_e at temperatures near T_c^- have not revealed any evidence for a second Bragg peak appearing at finite Q . On the other hand, changes in the order of 5% in the intensity of the Bragg peak at $Q = (1, 1/2, 0)$, associated with the 5 K transition, were observed and taken as evidence for a coupling of superconducting and antiferromagnetic order parameters.^{34,35}

This notion of coupling brings us to the third possible explanation, namely that the transition at T_c^- is superconducting by nature (i.e., it corresponds to the appearance of a new superconducting order parameter), and that it is brought about by the existing antiferromagnetic order. From the purely empirical point of view, we believe such a possibility, along with a fourth scenario where T_c^- is superconducting but not fundamentally related to magnetism, to be more likely than the second. The main argument is the sudden increase in the slope of $H_{c_1}(T)$ right at T_c^- , observed for both field directions ($H \perp c$ and $H \parallel c$) by Vincent and co-workers³² (for preliminary results, see Ref. 18), since this represents most likely an increase in the density of superconducting electrons. This feature is in fact a third thermodynamic “signature” for the lower transition.

In an attempt to account for a multiplicity of superconducting phases in UPt_3 as arising from a coupling to antiferromagnetism, two approaches have been developed. The first, initiated by Joynt,¹⁵ centers on the fact that ordered moments lying in the basal plane of the crystal structure break the hexagonal symmetry. In an even parity ground state, degeneracy can be lifted by a symmetry-breaking field. So, for example, the doubly degenerate transition to the E_{1g} representation is split by such a field, giving rise to

two transitions even in zero magnetic field, as shown by several authors.¹⁵⁻¹⁷ The splitting ΔT_c is then proportional to the strength of the field. The small separation of T_c^- and T_c^+ observed in UPt_3 is certainly suggestive of a splitting mechanism in general and, particularly, of a magnetic origin in view of the weak ordered moment. However, there is one general difficulty with the symmetry-breaking field model: it predicts—quite naturally—a highly anisotropic phase diagram, which is not what recent experiments have come to reveal. In qualitative terms, not only is the phase diagram relatively insensitive to an orientation of the magnetic field in and out of the basal plane, as shown in Sec. 3, but the $H_{c2}(T)$ curve is essentially independent of field direction in the basal plane,^{18,37,38} opposing the idea of a preferred direction defined, as supposed, by the sublattice magnetization. While one can perhaps get away with the kink occurring independent of the orientation of the field in the basal plane, by invoking a negligible magnetocrystalline anisotropy energy (not unlikely for such small moments in a hexagonal plane), the same argument can certainly not be applied to the near isotropy out of the basal plane. In other words, if there is a broken symmetry, why doesn't it manifest itself in any direct way?

Another “magnetic” scenario, proposed by Joynt and co-workers,³⁶ gets rid of the problem of “missing” anisotropy by focusing not on broken symmetry but rather on the unusual fact that in UPt_3 the magnetic order extends only over distances of about 150 Å, as measured by the width of the magnetic Bragg peak compared to the nuclear peak.¹⁴ Such a finite range is therefore comparable to the superconducting coherence length (of order 100 Å). In their model of a “superconducting glass,” in which the local magnetization has constant amplitude but random orientation, the authors preserve the microscopic mechanism of coupled order parameters while averaging for the macroscopic properties that thereby lose the anisotropy of broken macroscopic symmetry. A kink and a splitting are predicted, both strongly dependent on the amplitude of the moment.³⁶

Studies of the pressure dependence of the kink,²⁵ the splitting,²⁶ and the antiferromagnetic moment^{18,39} will offer the possibility of testing the “magnetic” scenario. In qualitative support of it, all three quantities are found to be strongly suppressed by hydrostatic pressure. However, the results are still too preliminary to establish in detail a strict correlation.¹⁸ Therefore other scenarios not based on a coupling to the magnetic order parameter are in principle just as valid. Examples of this type which have been put forward are (1) the splitting of two one-dimensional representations within the odd-parity scheme, by a weak spin-orbit coupling in the basal plane,³⁶ and (2) the accidental degeneracy between a one- and two-dimensional representation within the even-parity scheme, split by the crystal field.³⁶

5. CONCLUSION

We have investigated the double transition in the superconducting state of hexagonal UPt_3 . A phase diagram has been established by means of resistivity, specific heat, and thermal expansion measurements in a magnetic field applied parallel to the hexagonal axis. Within the experimental uncertainty the two thermodynamic measurements result in the same phase diagram with $dH_{c_2}^+/dT = -75$ and $dH_{c_2}^-/dT = -95$ kOe/K. The phase boundaries tend to merge at a critical point (or region) around $H^* = 8$ kOe, $T^* = 0.36$ K. Careful resistivity measurements of $H_{c_2}(T)$ show a discontinuity in the slope at $H = 6$ kOe and $T = 0.455$ K.

The new results imply that the two phase diagrams of UPt_3 for $H\parallel c$ and $H\perp c$ (Ref. 12) have the same general features. The low-field, low-temperature phase seems unaffected by the direction of the external applied field and is much less pressure dependent than the low-field, high-temperature phase. The here reported phase diagram for $H\parallel c$ is different than the one predicted theoretically, implying that the case of unconventional superconductivity in UPt_3 is certainly not solved. Hence, more theoretical and experimental work will follow in the near future.

ACKNOWLEDGMENTS

The work of A. d.V. has been made possible by a fellowship of the Royal Netherlands Academy of Arts and Sciences. K.H. thanks the Commission of the European Community (DG XII-CCR) for support. A.L. is supported by the CNPq (Conselho Nacional de Desenvolvimento Científico e Tecnológico, Brazil). K.B. is grateful to the French "Ministère de la Recherche et de la Technologie" for his scholarship.

REFERENCES

1. G. R. Stewart, Z. Fisk, J. Willis, and J. L. Smith, *Phys. Rev. Lett.* **52**, 679 (1984).
2. D. J. Bishop, C. M. Varma, B. Batlogg, and E. Bucher, *Phys. Rev. Lett.* **53**, 1009 (1984); B. S. Shivaram, Y. H. Jeong, T. F. Rosenbaum, and D. G. Hinks, *Phys. Rev. Lett.* **56**, 1078 (1986).
3. A. Sulpice, P. Gandit, J. Chaussy, J. Flouquet, D. Jaccard, P. Lejay, and J. L. Tholence, *J. Low Temp. Phys.* **62**, 39 (1986).
4. D. Jaccard, J. Flouquet, P. Lejay, and J. L. Tholence, *J. Appl. Phys.* **57**, 3082 (1985).
5. Y. Kohori, T. Kohara, H. Shibai, Y. Oda, Y. Kitaoka, and K. Asayama, *J. Phys. Soc. Jpn.* **57**, 395 (1988).
6. U. Rauchschwalbe, U. Ahlheim, F. Steglich, D. Rainer, and J. J. M. Franse, *Z. Phys. B* **60**, 379 (1985).
7. L. Taillefer, F. Piquemal, and J. Flouquet, *Physica C* **153-155**, 451 (1988).
8. V. Müller, Ch. Roth, D. Maurer, E. W. Scheidt, K. Lüders, E. Bucher, and H. E. Bömmel, *Phys. Rev. Lett.* **58**, 1224 (1987).
9. Y. J. Qian, M.-F. Xu, A. Schenstrom, H.-P. Baum, J. B. Ketterson, D. Hinks, M. Levy, and B. K. Sarma, *Solid State Commun.* **63**, 599 (1987).

10. A. Schenstrom, M.-F. Xu, Y. Hong, D. Bein, M. Levy, B. K. Sarma, S. Adenwalla, Z. Zhao, T. Tokuyasu, D. W. Hess, J. B. Ketterson, J. A. Sauls, and D. G. Hinks, *Phys. Rev. Lett.* **62**, 332 (1989).
11. R. A. Fisher, S. Kim, B. F. Woodfield, N. E. Phillips, L. Taillefer, K. Hasselbach, J. Flouquet, A. L. Giorgi, and J. L. Smith, *Phys. Rev. Lett.* **62**, 1411 (1989).
12. K. Hasselbach, L. Taillefer, and J. Flouquet, *Phys. Rev. Lett.* **63**, 93 (1989).
13. H. R. Ott, H. Rudigier, Z. Fisk, J. L. Fisk, and J. L. Smith, *Phys. Rev. B* **31**, 1651 (1985).
14. G. Aeppli, E. Bucher, C. Broholm, J. K. Kjems, J. Baumann, and J. Hufnagl, *Phys. Rev. Lett.* **60**, 615 (1988).
15. R. Joynt, *Supercond. Sci. Technol.* **1**, 210 (1988).
16. K. Machida, M. Ozaki, and T. Ohmi, *J. J. Phys. Soc. Jpn.* **58**, 4116 (1989).
17. D. W. Hess, T. Tokuyasu, and J. A. Sauls, *J. Phys. Cond. Mat.* **1**, 8135 (1989).
18. L. Taillefer, K. Behnia, K. Hasselbach, J. Flouquet, S. M. Hayden, and C. Vettier, in *The Proceedings of the XXV Yamada Conference, Osaka, April, 1990* (to be published).
19. K. Hasselbach, L. Taillefer, and J. Flouquet, in *The Proceedings of the 19th Conference on Low Temperature Physics, Brighton, August, 1990* (to be published).
20. L. Taillefer, *Physica B* **163**, 280 (1990).
21. B. Ellman, J. Yong, T. F. Rosenbaum, and E. Bucher, *Phys. Rev. Lett.* **64**, 1569 (1990).
22. A. de Visser, A. Menovsky, J. J. M. Franse, K. Hasselbach, A. Lacerda, L. Taillefer, P. Haen, and J. Flouquet, *Phys. Rev. B* **41**, 7304 (1990).
23. A. de Visser, Ph.D. Thesis, University of Amsterdam (1986, unpublished).
24. M. Greiter, L. Taillefer, N. Austin, and C. G. Lonzarich, in *The Proceedings of the International Conference on Valence Fluctuations, Rio de Janeiro, July 1990* (to be published).
25. K. Behnia, L. Taillefer, and J. Flouquet, *J. Appl. Phys.* **67**, 5200 (1990).
26. Th. Trappmann and H.v. Löhneysen, to be published.
27. R. N. Kleinmann, P. L. Gammel, E. Bucher, and D. J. Bishop, *Phys. Rev. Lett.* **62**, 328 (1989).
28. K. Behnia, L. Taillefer, J. Flouquet, D. Jaccard, and Z. Fisk, in *The Proceedings of the 19th Conference on Low Temperature Physics, Brighton, August, 1990* (to be published).
29. G. J. C. L. Bruls, D. Weber, B. Wolf, B. Lüthi, A. A. Menovsky, A. de Visser, and J. J. M. Franse, in *The Proceedings of the 19th Conference on Low Temperature Physics, Brighton, August, 1990* (to be published).
30. G. E. Volovik, *J. Phys. C* **21**, L221 (1988).
31. T. Vorenkamp, Z. Tarnavski, H. P. van der Meulen, K. Kadowaki, V. J. M. Meulenbroek, A. A. Menovsky, and J. J. M. Franse, *Physica B* **163**, 584 (1990).
32. E. Vincent, J. Hammann, L. Taillefer, K. Behnia, N. Keller, and J. Flouquet, to be published.
33. H. C. Hamaker, L. D. Woolf, H. B. McKay, Z. Fisk, and M. B. Maple, *Solid State Commun.* **32**, 289 (1979).
34. G. Aeppli, D. Bishop, C. Broholm, E. Bucher, K. Siemensmayer, M. Steiner, and N. Stüsser, *Phys. Rev. Lett.* **63**, 676 (1989).
35. E. I. Blount, C. M. Varma and G. Aeppli, *Phys. Rev. Lett.* **64**, 3074 (1990).
36. R. Joynt, V. P. Mineev, G. E. Volovik, and M. E. Zhitomirsky, *Phys. Rev. B* (submitted).
37. B. S. Shivaram, T. F. Rosenbaum, and D. G. Hinks, *Phys. Rev. Lett.* **57**, 1259 (1986).
38. T. Vorenkamp, A. de Visser, R. Wester, A. A. Menovsky, and J. J. M. Franse, in *The Proceedings of the 19th Conference on Low Temperature Physics, Brighton, August, 1990* (to be published).
39. S. M. Hayden, C. Vettier, L. Taillefer, and J. Flouquet, to be published.